

# LJMU Research Online

Asteris, PG, Sivenas, T, Gkantou, M, Formisano, A and Le, TT

Estimation of axial load-carrying capacity of elliptical concrete filled steel tubular columns using computational intelligence

https://researchonline.ljmu.ac.uk/id/eprint/27394/

## Article

**Citation** (please note it is advisable to refer to the publisher's version if you intend to cite from this work)

Asteris, PG ORCID logoORCID: https://orcid.org/0000-0002-7142-4981, Sivenas, T, Gkantou, M ORCID logoORCID: https://orcid.org/0000-0003-2494-405X, Formisano, A ORCID logoORCID: https://orcid.org/0000-0003-3592-4011 and Le. TT (2025) Estimation of axial load-carrying capacity of

LJMU has developed LJMU Research Online for users to access the research output of the University more effectively. Copyright © and Moral Rights for the papers on this site are retained by the individual authors and/or other copyright owners. Users may download and/or print one copy of any article(s) in LJMU Research Online to facilitate their private study or for non-commercial research. You may not engage in further distribution of the material or use it for any profit-making activities or any commercial gain.

The version presented here may differ from the published version or from the version of the record. Please see the repository URL above for details on accessing the published version and note that access may require a subscription.

For more information please contact <a href="mailto:researchonline@ljmu.ac.uk">researchonline@ljmu.ac.uk</a>

Contents lists available at ScienceDirect

# Journal of Building Engineering

journal homepage: www.elsevier.com/locate/jobe





# Estimation of axial load-carrying capacity of elliptical concrete filled steel tubular columns using computational intelligence

Panagiotis G. Asteris <sup>a,\*</sup>, Tryfon Sivenas <sup>a</sup>, Michaela Gkantou <sup>b</sup>, Antonio Formisano <sup>c</sup>, Tien-Thinh Le <sup>d,e</sup>

- <sup>a</sup> Computational Mechanics Laboratory, School of Pedagogical and Technological Education, Marousi, 14121, Athens, Greece
- <sup>b</sup> School of Civil Engineering and Built Environment, Liverpool John Moores University, Liverpool, L3 3AF, UK
- c Department of Structures for Engineering and Architecture, School of Polytechnic and Basic Sciences, University of Naples "Federico II", P.le V. Tecchio, 80125, Naples, Italy
- d Faculty of Mechanical Engineering and Mechatronics, PHENIKAA University, Yen Nghia, Ha Dong, Hanoi, 12116, Viet Nam
- e PHENIKAA Research and Technology Institute (PRATI), A&A Green Phoenix Group JSC, No.167 Hoang Ngan, Trung Hoa, Cau Giay, Hanoi, 11313, Viet Nam

### ARTICLE INFO

#### Keywords:

Elliptical concrete filled steel tube (ECFST) Artificial neural networks (ANNs) Computational intelligence Optimization algorithm Ultimate axial load

#### ABSTRACT

Elliptical Concrete Filled Steel Tubular (ECFST) members exhibit superior aesthetics and improved structural performance in certain applications. However, accurately estimating their axial load-carrying capacity remains a challenge due to the complex interaction between geometric parameters and material strengths. This study presents a computational intelligence-based approach to predict the axial load-carrying capacity of ECFST members using hybrid artificial neural networks (ANN) and metaheuristic optimization techniques. A comprehensive dataset comprising 500 structural performance literature data has been initially collated. The dataset incorporates key geometry and material parameters, covering a wide range of material strengths and cross-sectional and member geometrical dimensions, A total of 1,555,200 different ANN architectures were trained using global optimization algorithms to deduce the optimum condition. The performance of the optimum model is also compared to current design standards, including European, American and Chinese codes. Assessment of the key parameters influencing the axial load-carrying capacity is also done using SHapley Additive exPlanations (SHAP). For practical application, a matrix form explicit equation and a Graphical User Interface are also derived based on the optimum prediction model and provided as supplementary material to the interested researchers.

## Nomenclature

2a 2bANN(s) ANN-BFGS ANN-ICA ANN-I.M

Larger diameter of an elliptical section Smaller diameter of an elliptical section

Artificial Neural Network(s)

Artificial Neural Network optimized by Broyden-Fletcher-Goldfarb-Shanno quasi-Newton algorithm Artificial Neural Network optimized by Imperialist Competitive Algorithm

Artificial Neural Network optimized by Levenberg-Marquardt algorithm

(continued on next page)

E-mail address: panagiotisasteris@gmail.com (P.G. Asteris).

https://doi.org/10.1016/j.jobe.2025.113738

Received 8 April 2025; Received in revised form 10 July 2025; Accepted 12 August 2025 Available online 15 August 2025

2352-7102/© 2025 The Authors. Published by Elsevier Ltd. This is an open access article under the CC BY license (http://creativecommons.org/licenses/by/4.0/).

Corresponding author.

#### (continued)

ANN-PSO Artificial Neural Network optimized by Particle swarm algorithm
BFGS Broyden–Fletcher–Goldfarb–Shanno quasi-Newton algorithm

BPNN Back Propagation Neural Network
Co Competitive transfer function

Compet ECFST MATLAB function for the Competitive (Co) transfer function Elliptical Concrete Filled Steel Tube

 $f_c$  Concrete cylinder compressive strength [in MPa]

Yield strength of steel [in MPa]

hardlim MATLAB function for the Hard-limit (HL) transfer function

hardlims MATLAB function for the Symmetric hard-limit (SHL) transfer function

Length of column

ICA Imperialist Competitive Algorithm
Li Linear transfer function
LM Levenberg-Marquardt algorithm

logsig MATLAB function for the Log-sigmoid (LS) transfer function

LS Log-Sigmoid transfer function
MAPE Mean Absolute Percentage Error
MSE Mean Square Error

NRB Normalized Radial Basis transfer function  $N_u$  Axial Load-Carrying Capacity [in kN] PLi Positive Linear transfer function

poslin MATLAB function for the Positive linear (PLi) transfer function

PSO Particle Swarm Optimization algorithm

purelin MATLAB function for the Linear (Li) transfer function

Pearson correlation coefficient

RA Regression Analysis

radbas MATLAB function for the Radial basis (RB) transfer function

radbasn MATLAB function for the Normalized radial basis (NRB) transfer function

RB Radial Basis transfer function

satlin MATLAB function for the Saturating linear (SL) transfer function

satlins MATLAB function for the Symmetric saturating linear (SSL) transfer function

SM Soft Max transfer function

softmax MATLAB function for the Soft max (SM) transfer function

SSE Sum Square Error

SSL Symmetric Saturating Linear transfer function

TB Triangular Basis transfer function

tansig MATLAB function for the Hyperbolic Tangent Sigmoid (HTS) transfer function

Thickness of steel tube

tribas MATLAB function for the Triangular basis (TB) transfer function

## 1. Introduction

Concrete-filled steel tubular (CFST) columns are increasingly used in modern construction due to their structural benefits and practical advantages. These columns consist of a structural steel hollow steel, which may be hot-rolled, cold-formed, or welded, infilled with concrete. This composite system offers multiple benefits. The steel tube functions as formwork, eliminating the need for additional formwork and thus reducing labour costs and increasing the speed of construction. It also provides confinement for the infill concrete, enhancing its compressive strength and ductility. In addition, the concrete core provides a restraint to the steel tube against local buckling, allowing the use of more slender steel sections without compromising stability. Overall, a composite CFST column can achieve enhanced stiffness, strength, and ductility, outperforming its individual components and thus it often finds applications in high rise buildings. Further advantages include increased useable floor space and enhanced fire resistance.

Elliptical concrete-filled hollow sections (ECFST) have attracted significant interest in recent years due to their aesthetic appeal and structural efficiency. In particular, the bending capacity of an ECFST is different in the major and the minor axis, and thus the design can be tailored to the project's requirements, whilst the elliptical shape allows for considerable aesthetic values. As with other cross-sectional shapes, the composite action between the steel tube and the concrete leads to enhanced structural efficiency. The degree of confinement provided by an elliptical section lies between that of circular sections (offering uniform confinement) and rectangular sections (providing limited confinement), with the aspect ratio of the elliptical profile influencing this effect. Research has investigated the structural behaviour of members made from ECFST under various loading conditions. Stub columns aiming at investigating the compressive cross-sectional resistance and characterised by their small height relative to their cross-sectional dimensions, have been the focus of several studies. Examples include the experimental study of [1] who investigated axially loaded stainless steel elliptical stub columns filled with concrete, whereas [2] proposed a new design equation based on their experimental findings for ECFST stub columns. In contrast to stub columns, slender columns have a greater height-to-cross-section ratio, making them more susceptible to flexural buckling failure modes and require different design considerations [3]. examined the flexural buckling behaviour under both the major and minor axes of ECFST columns [4]. studied cold-formed ECFST members with varying aspect ratios, whilst [5] assessed the performance of columns made from commercially available elliptical steel hollow sections filled with self-compacting concrete.

Recent advances in computational intelligence and numerical modelling have significantly improved structural analysis and damage detection in complex systems [6–8]. Nowadays, the artificial neural network (ANN) method has steadily gained popularity and found applications across various fields in structural engineering [9] and in particular for strength prediction of structural members.

ANN method uses experimental data to train neural networks, enabling them to generalize and predict the capacity of structural members under various loading scenarios. Recent research studies have explored its application in estimating the performance of composite steel-concrete columns. Specifically, for ECFST, the application of soft computing techniques will be of great significance, given that many of the current international design codes do not provide a methodology specifically for an elliptical concrete-filled steel tubular section, as will be briefly explained in Section 2. Section 2 also highlights the limited research on computational intelligence models for ECFSTs.

This study addresses a critical gap in the strength prediction of ECFST columns. The complex geometry of the elliptical composite cross-section presents challenges for accurate strength prediction, making conventional design methods less effective for ECFSTs. To overcome these limitations, the application of soft computing techniques is proposed as a promising solution. This research introduces a novel approach that employs computational intelligence techniques to estimate the axial load-carrying capacity of ECFST columns, supported by a comprehensive database of structural performance data. The proposed method enhances prediction accuracy, while effectively addressing the scarcity of research involving artificial intelligence-based approaches for ECFSTs. These columns could offer a unique combination of structural and architectural advantages compared to rectangular and circular composite sections. In particular, they provide improved load distribution compared to rectangular sections, while offering greater directional strength efficiency than circular ones. Architecturally, their sleek, space-efficient shape enhances modern designs with an elegant, streamlined appearance and greater aesthetic appeal in contemporary infrastructure. The approach developed in this study not only enables more accurate strength prediction of ECFST columns but also promotes their broader adoption in advanced structural applications.

The paper is structured as follows. Upon presenting a brief overview of relevant structural design standards and recent research on soft computing models for CFST in Section 2, the materials and methods applied herein are presented in Section 3. The obtained results are analysed in Section 4, whilst limitations and future research directions, and conclusions are provided in Sections 5 and 6, respectively. This paper is supplemented with the following additional material: A) Parameters of ANNs; B) An Excel file titled 'Top 20 ANN Architectures'; and C) An Excel file titled 'Final Values of Weights and Biases' for interested readers.

# 2. Short review on standards and soft computing models for the axial load-carrying capacity of concrete-filled steel tubular columns

### 2.1. Design codes for ECFST columns

Existing design codes generally lack specific provisions for elliptical concrete-filled steel tubular sections despite their potential structural and architectural advantages. In most cases, codes refer to the general case of composite cross-sections or to circular or "round" filled sections. This is mainly because limited research has focused on elliptical shapes, compared to the extensive experimental data available for circular and rectangular sections. The complex geometry of elliptical sections leads to unique stress distributions that are difficult to model and standardize, which motivates the development of our computational intelligence model. Additionally, their relatively limited widespread use contributes to the absence of simplified applicable design rules, leaving a gap in current codes that this study aims to address.

This section provides a brief overview of the design recommendations for predicting the axial load-carrying capacity of ECFST columns as outlined in the design codes considered in this study. It is noted that all safety factors for the assessments presented in Section 4 have been taken as unity. Furthermore, each of these codes provides limits for the maximum strength of steel and concrete, allowable cross-sectional and member slenderness, steel contribution percentage, and others. The assessment and consideration of the application of these limits have been excluded from the scope of this study. It is important to note that any deviations from code limits may occur due to the properties of the original experimental data, which were beyond the authors' control; nevertheless, their inclusion broadens the dataset and enhances the model's generality.

## 2.1.1. European code

According to the simplified method of EN 1994-1-1 [10] (EC4), the axial load-carrying capacity ( $N_{EC4}$ ) of a composite concrete-filled steel hollow section column can be determined by multiplying the cross-sectional compression resistance ( $N_{pl}$ ) by a reduction factor ( $\chi$ ) to account for flexural buckling (see Eq. (1)). The cross-section's compression plastic resistance considers the contributions of the steel and concrete materials, according to Eq. (2). In order to calculate the buckling reduction factor  $\chi$ , EN 1994-1-1 [10] suggests using the nondimensional member slenderness  $\bar{\lambda}$  from Eq. (3). Based on this value, the reduction factor,  $\chi$ , is then determined according to the buckling curves specified in EN 1993-1-1 [11]. The nondimensional slenderness  $\bar{\lambda}$  depends on the values of the plastic compressive resistance over the elastic critical buckling load ( $N_{cr}$ ). The latter is determined using the effective flexural stiffness, considering the Elastic Modulus ( $E_s$ ,  $E_c$ ) and moment of inertia ( $I_s$ ,  $I_c$ ) in the relevant buckling axis, of the steel and concrete, respectively, as defined in Eq. (4).

$$N_{EC4} = \chi N_{pl} \tag{1}$$

$$N_{pl} = f_y A_{s_+} f_c A_c \tag{2}$$

$$\overline{\lambda} = \sqrt{\frac{N_{pl}}{N_{cr}}} \tag{3}$$

$$EI_{eff} = E_s I_s + 0.6 E_c I_c \tag{4}$$

Elliptical sections provide confinement levels between circular and rectangular sections, influenced by their aspect ratio. It is noteworthy that in EN 1994-1-1 [10], there is no explicit formula for elliptical concrete-filled steel tubular sections. Therefore, herein we will consider and assess the following cases.

- 2.1.1.1. Generic equation for composite steel-concrete cross-sections. Eq. (2) is the generic formula provided in Section 6.7.3.2 of EN 1994-1-1 [10] for calculating the plastic resistance of concrete-filled cross-sections, by summing the strengths of their components, and hence the applicability of this equation to ECFST columns is assessed.
- 2.1.1.2. Equation for circular concrete-filled hollow sections. For circular concrete-filled steel hollow sections, EN 1994-1-1 [10] (Clause 6.7.3.2(6)) recommends using Eq. (5) instead of Eq. (2) to account for the confinement provided to the concrete by the circular shape. The applicability of this formula to elliptical hollow sections has been discussed in the literature and will also be presented here.

$$N_{pl} = n_s f_y A_{s+} f_c A_c \left( 1 + \frac{n_c t f_y}{f_c} \right)$$
 (5)

where  $n_s$ ,  $n_c$  coefficients defined in EN 1994-1-1 [10], D the cross-sectional diameter,  $A_s$  and  $A_c$  are the cross-sectional areas of steel and concrete, respectively, t is the thickness of the steel section, and  $f_c$  and  $f_y$  are the compressive cylinder strength of the concrete and the yield strength of the steel, respectively. It is noteworthy that herein the subscript s stands for the elliptical structural steel, whilst there are no reinforcement bars in the examined concrete-filled steel sections.

2.1.1.3. Jamaluddin (2013). Ref. [5] suggests using the design equations from EN 1994-1-1 [10] for circular concrete-filled steel hollow sections (i.e., Eq. (5)), but recommends considering confinement at the cross-sectional level by using the equivalent diameter ( $D_e$ ) proposed by Ref. [12] (Eq. (6)), as the cross-sectional diameter of the elliptical section.

$$D_e = 2a^2/b \tag{6}$$

2.1.1.4. Liu et al [13]. Ref. [13] have suggested the same approach as [5], either using the equivalent diameter from Eq. (6), or, alternatively, using the equivalent diameter equation proposed by Ref. [14] (Eq. (7)). This second recommendation will also be assessed here.

$$D_e = 2a \left[ 1 + f \left( \frac{a}{b} - 1 \right) \right] \tag{7}$$

where f as defined in by [14].

2.1.1.5. Second generation of BS EN 1994-1-1 (draft, 2024). It is noteworthy that the draft version of the second-generation EC4 is available at the time of writing, and it specifies that non-typical cross-sections, such as elliptical sections, are excluded from the simplified method using design equations, described in Section 2.1.1. It is thus recommended that ECFST columns should be verified using the general method. This would involve carrying out a non-linear analysis, accounting for factors such as residual stresses, geometrical imperfections, local instability, concrete cracking, creep, shrinkage, and the yielding of steel and covering all relevant failure modes and ensuring stability under the most unfavourable combination of actions. This is related to the complexity of predicting the ECFST column behaviour, due to the intricate nature of confinement in the elliptical shape. This complexity further underscores the relevance of our paper, which will use ANN and provide an empirical formula for the strength prediction of ECFST columns.

## 2.1.2. American code

AISC 360-10 [15] provides design recommendations for "round filled sections" without distinguishing between circular and elliptical shapes. It suggests accounting for the local buckling effects in composite cross-sections by initially classifying the steel tubes into three categories (compact, non-compact, slender), based on the D/t ratio of the steel tube. The nominal compressive capacity of the composite section ( $P_{no}$ ) is calculated according to this classification. Then, the load-carrying capacity of an axially loaded composite column, is determined as a function of both  $P_{no}$  and  $P_{cr}$ , from Eq. (8).  $P_{cr}$  is the Euler critical load, which is calculated using the effective stiffness of the column, considering the elastic moduli of both the steel and the concrete. The concrete's modulus is further multiplied by a coefficient C3 to account for the effective rigidity of the filled composite columns.

$$N_{AISC360} = \begin{cases} P_{no}\left(0.658^{\frac{P_{no}}{P_{cr}}}\right), if \frac{P_{no}}{P_{cr}} \le 2.25\\ 0.877P_{cr}, if \frac{P_{no}}{P_{cr}} > 2.25 \end{cases}$$
(8)

### 2.1.3. Chinese code

Among the current design codes for CFST columns, only the Chinese code GB50936 [16] addresses the design of ECFST columns. The load-carrying capacity of this column is determined by a reduction factor ( $\chi$ ), which adjusts the column's strength based on its slenderness ratio ( $\lambda_{cs}$ ). This slenderness ratio depends on geometry of the column (the steel area  $A_s$  and the concrete area  $A_c$ ) and the material properties  $f_{cs}$  (the compressive strength of the composite section). Compared to other codes,  $f_{cs}$ , is calculated as a function of coefficients B and C, which account for the cross-sectional aspect ratio b/a, thereby considering also the case of the elliptical shape for b/a larger than unity.

$$N_{\text{GB50936}} = \gamma f_{cs} \left( A_{s\perp} A_c \right)$$
 (9)

### 2.1.4. Uenaka [2]

Based on the results of 21 tests [2], suggested a design equation with a calibrated coefficient, for the prediction of the compressive capacity of ECFST cross-sections. The accuracy of this formula is assessed herein. Note this equation only refers to cross-sectional capacity (stub column data, as will be listed in Table 2) and therefore is relevant only to the 367 out of 500 data of this study.

$$N_{\text{Uenaka}} = 1.46 \left( f_{y} A_{s_{+}} f_{c} A_{c} \right) \tag{10}$$

## 2.2. Soft computing models for the axial load-carrying capacity of CFST columns

Soft computing techniques have emerged as powerful tools for solving complex engineering problems, particularly in structural analysis and design, as these models can effectively handle uncertainties, nonlinearities, and intricate interactions among the input space. In the context of CFSTs, these models offer an advanced alternative for estimating the axial load-carrying capacity. Table 1 lists research studies on the prediction of axial load-carrying capacity of CFST members using soft computing techniques. The table summarises the soft computing techniques used, the input parameters (geometry and material properties), the number of data points

Table 1
Research studies on the prediction of the axial load-carrying capacity of CFST columns using computational intelligence.

References	Model	Input parameters	Samples	Cross-Sectional shape	Accuracy (Coefficient of determination, R <sup>2</sup> )	Provided output
[17]	ANN	$B, H, t, L_e, f_y, f_c,$	1224	Rectangular	Training: 0.9853	Weights and biases, Formula and GUI
[18]	ANN	$D$ , $t$ , $L_e$ , $f_y$ , $f_c$	268	Circular	Testing: 0.9825 Training: 0.8767 Testing: 0.8676	-
[19]	ANN-FA	$B, H, t, L_e, f_y, f_c,$ $e$	1300	Rectangular	Training: 0.9868, Testing: 0.9884	Weights and biases, Formula and GUI
[20]	ANN	$B, H, t, L_e, f_y, f_c$	150	Rectangular	Training: 0.9999 Testing: 0.9899	-
[21]	Gene-Expression- Programming	$D, t, L_e, f_y, f_c$	314	Circular	0.9781	-
[22]	CATB, XGB	$2a, 2b, L, t, f_y,$ $f_c$	116	Elliptical	CATB: Training: 0.991 XGB: Training: 0.991 CATB: Testing: 0.967 XGB: Testing: 0.970	GUI
[23]	ANN-BCMO	$B, H, t, L_e, f_y, f_c$	880	Rectangular	Training: 0.9876 Testing: 0.9912	Weights and biases, Formula and GUI
[24]	ANN-BCMO	$D, t, L_e, f_y, f_c$	1245	Circular	Training: 0.9996 Testing: 0.9883	Weights and biases
[25]	ANFIS-PSO	$2a, 2b, L, t, f_y,$ $f_c$	222	Elliptical	Training: 0.936, Testing: 0.942	-
[26]	Fuzzy Logic	$D, t, L_e, f_y, f_c$	123	Circular	average error: 7.5 % standard deviation: 0.085	-
[27]	GBR, XGBR	$2a, 2b, L, t, f_y,$ $f_c$	180	Elliptical	GBR: Testing: 0.9888 XGBR: Testing: 0.9885	GUI
[28]	Hybrid feedforward neural network	$B, H, t, L_e, f_y, f_c$	99	Rectangular	Training: 0.978, Testing: 0.979	-
[29]	XGBoost	$2a$ , $2b$ , $L$ , $t$ , $f_y$ , $f_c$	119	Elliptical	Training: 0.999, Testing: 0.993	GUI
[30]	ANN	$D, t, L_e, f_y, f_c$	768	Circular	Training: 0.9999 Testing: 0.9999	Weights and biases, Formula and GUI
[31]	ANN	$D, t, L_e, f_y, f_c$	125	Hollow circular	0.995	Formula and GUI

2 $\alpha$ : Larger diameter; 2b: Smaller diameter; B: Cross-sectional width H: Cross-sectional depth;  $f_y$ : Yield strength of steel;  $f_c$ : Concrete compressive strength L: Length of column;  $L_e$ : Effective length of column; t: Thickness of steel tube, e: Eccentricity of applied axial load; ANN: Artificial Neural Network; ANN-FA: Artificial Neural Network optimized by Firefly algorithm; FA: Firefly algorithm; ANFIS: Adaptive neuro-fuzzy inference systems; ANFIS-PSO: Adaptive neuro-fuzzy inference systems optimized by Particle swarm optimization; PSO: Particle swarm optimization.

**Table 2**Data from published in literature.

Nr.	Reference	Number of Test Samples	Section	Axial Load-Carrying Capacity in kN	Type of Columns
1	[2]	21	Elliptical	389.10–921.30	stub columns
2	[4]	5	Elliptical	728.00-1376.00	stub & slender columns
3	[13]	18	Elliptical	687.20-2607.00	stub columns
4	[33]	3	Elliptical	1139.00-1862.50	slender columns
5–6	[5,34]	24	Elliptical	326.60-2116.00	slender columns
7	[32]	64 FE	Elliptical	111.00-8641.00	slender columns
8	[35]	9	Elliptical	839.00-1483.00	stub columns
9	[3]	7	Elliptical	349.00-1176.90	stub & slender columns
10	[36]	8	Elliptical	1075.00-2290.00	stub columns
11	[37]	2	Circular	1051.50-1292.10	slender columns
12	[38]	2	Circular	996.00-1008.00	stub columns
13	[39]	8	Elliptical	556.00-2184.00	slender columns
14	[40]	12	Circular & Elliptical	843.00-1450.00	stub columns
15	[41]	4	Circular	1428.32-2511.30	stub columns
16	[42]	13	Elliptical	663.00-1479.00	stub columns
17	[1]	6	Elliptical	412.30-1064.80	stub columns
18	[43,44]	11	Circular	1875.00-3930.00	stub columns
19	[45]	3	Circular	2013.00-3015.00	stub columns
20	[46]	3	Circular	881.00-2715.00	stub columns
21	[47]	5	Circular	2182.00-2513.00	stub columns
22	[48]	23	Circular	107.60-11661.90	stub & slender columns
23	[49]	9	Circular	633.26-1212.90	stub columns
24	[50]	11	Circular	1104.10-2599.60	stub columns
25	[51]	4	Circular	4545.00-7280.20	stub columns
26	[52]	13 (& 50 FE)	Elliptical	560.60-18187.90	stub columns
27	[53]	2	Elliptical	1254.00-2588.00	stub columns
28	[54]	18	Elliptical	2622.80-4143.55	stub columns
29	[55]	7 (& 96 FE)	Elliptical	741.00–37494.00	stub columns
30	[56]	6	Elliptical	1897.27-3600.53	stub columns
31	[13]	18	Elliptical	687.20–2607.00	stub columns
	Total	500	354 Elliptical 146 Circular	107.60–37494.00	367 stub columns 133 slender columns

used for the model development, the cross-sectional shape of the column, the values of coefficient of determination for training and for testing, as well as the provided output, such as the weights and bias of models, provided formula or/and graphical user interface (GUI). It is seen that different cross sections for the CFST members have been investigated, including circular, rectangular (square) and elliptical. In terms of number of data points, the smallest size of dataset is 99 and the largest number of data points is 1300. Different soft computing techniques have been employed, including Artificial Neural Network, Gene-Expression-Programming, Gradient Boosting, eXtreme Gradient Boosting, CatBoost and Fuzzy Logic. Besides, various global optimizations have been integrated to deduce the optimum ANN model, such as Firefly Algorithm, Balancing Composite Motion Optimization and Particle Swarm Optimization. It can be stated that for CFST members, soft computing techniques can learn from experimental/numerical data and predict axial load-carrying capacity based on geometrical and material parameters.

It is observed that existing research on CFSTs members primarily focuses on circular and rectangular sections, with empirical formulas derived based on regression analysis and graphical user interface. However, for elliptical sections, to the best of the authors' knowledge, no studies have proposed an empirical prediction equation that explicitly incorporates the details of model weights and biases. Moreover, deeper analysis and comparisons with current design standards are essential to assess the applicability of computational intelligence models to ECFSTs.

## 3. Materials and methods

This section presents the methodology followed for the development and formulation of a computational mathematical model for estimating the axial load-carrying capacity of elliptical concrete-filled steel tubular columns, as well as the database used for the training, development, and validation of the model. Special emphasis is given to the compilation of the experimental database and the parameters used to simulate the behaviour of the columns, particularly those parameters that influence its axial load-carrying capacity. Additionally, the methodology and computational techniques employed to formulate the optimal model are thoroughly and deeply discussed.

## 3.1. Compilation of the database

It is common practice for most researchers involved in the formulation and development of predictive computational models to focus more on the computational methods and techniques used, and less on the database used for the development, training, and testing of the model's performance and reliability. The authors of this paper firmly believe the opposite. We consider that the primary

factor determining the reliability of a predictive computational model lies in the accuracy and comprehensiveness of the database used to describe the phenomenon under study, without neglecting the importance of the computational method. No matter how innovative or advanced a computational technique is, it cannot lead to a reliable predictive model unless it is supported by a reliable and representative database. This underlines and reaffirms the well-known adage from computer science: "garbage in, garbage out."

Given the importance of the database, it is considered useful and appropriate to briefly present the key principles that should be followed when compiling a reliable and comprehensive database. A reliable database consists of true and trustworthy data while also ensuring that the data adequately and statistically cover all possible values that each variable in the studied problem can take. Furthermore, when collecting experimental data, it is crucial to select data from experiments conducted in certified and credible laboratories, adhering to all relevant international standards, including the preparation and storage of specimens under appropriate environmental conditions.

Based on the above considerations, a comprehensive experimental database was compiled to develop and formulate an optimal and reliable computational model for estimating the axial load-carrying capacity of ECFST columns. This database consists of 500 data points collected from 31 published experimental studies, which are listed in Table 2. It is worth mentioning that 30 out of the 31 publications whose data were used for the composition of the database include experimental studies, while only one [32] is a purely numerical study, in which the axial load-carrying capacity of 64 columns is examined using the finite element (FE) method. To the best of the authors' knowledge and according to Table 1, this experimental database is the largest ever compiled and used for studying the axial load-carrying capacity of concrete-filled steel tubes with elliptical hollow sections. The database is defined by seven parameters, six of which are input parameters, while the seventh is the output parameter, representing the axial load-carrying capacity. In Table 2, besides the authors of each study used for the compilation of the database, the number of samples, the range of axial load-carrying capacity values studied and the type of the columns based on their relative member slenderness (stub/slender columns) are also provided. Note the authors used the ratio of column length to the smaller cross-sectional dimension (L/2b), corresponding to the critical buckling axis of the elliptical section, to capture sensitivity to buckling effects. This ratio, expressed as 2 b/L and included as an input parameter, was selected as the slenderness measure due to its simplicity and reliable performance. To improve the accuracy and applicability of the ANN model outlined in Section 4 and given the relatively limited number of ECFST data available in the literature, the database has also included a proportion of circular CFST columns, representing the case where the two diameter input parameters are equal (2a = 2b).

At this point, it is worth further discussing the parameters (input parameters for the trained and developed computational intelligence models) that were selected as capable of simulating the behaviour of steel tubes and, consequently, influencing the value of the axial load-carrying capacity  $(N_u)$ , which is the output parameter of the model.

Following the emphasis placed earlier on the necessity of a reliable and capable database, the selection of the parameters that compose the database, is also included. In fact, the way in which the parameters are chosen, as well as their number, affects the entire process of training and developing the predictive computational intelligence model. The number of parameters should be minimised while still being sufficient to describe the problem under study.

In this context, the six parameters used, in the order in which they define each dataset of the database, are: the two diameters of the elliptical section, namely the larger diameter of the elliptical cross-section relevant to the major axis (2a) and the smaller diameter of the elliptical cross-section relevant to the minor axis (2b); the thickness of the steel tube (t); the yield strength of steel  $(f_y)$ ; the concrete cylinder compressive strength  $(f_c)$ ; and the ratio (2b/L) to consider the member slenderness.

Table 3 presents the aggregated statistical data for the entire database compiled from the 31 experimental studies listed in Table 2. Specifically, the table shows the minimum (Min), average, and maximum (Max) values, as well as the Standard Deviation (STD) and Coefficient of Variation (CV) for each parameter involved in the problem, which determines the axial compassion capacity of concrete-filled steel tubes with elliptical hollow sections. In addition to the statistical parameters, Fig. 1 displays the histograms of the parameters used for predicting the axial load-carrying capacity. Fig. 1(a) and (b) show the cross-sectional diameters of the elliptical sections, demonstrating a good range varying from smaller values to diameters of up to 570 mm. Fig. 1(c) presents the thicknesses of the steel tube ranging from 0.9 mm to 26 mm. As shown in these figures and as anticipated, there is an increasing trend of the load-carrying capacity with larger cross-sectional diameters and thicknesses. The material strengths of the collated dataset are presented in Fig. 1(d) and (e). The majority of the studies have focused on conventionally used steel grades, with an average value of 379.03 MPa, whilst higher strength values have been considered for both materials with values up to 834 MPa and 120 MPa for the steel and concrete, respectively. The present study aims to propose one uniform model for predicting the load-carrying capacity of composite

**Table 3**Statistics of the parameters involved in predicting Axial Load-carrying Capacity.

Nr.	Variable	Symbol	Unit	Category	Statistics				
					Min	Average	Max	STD	CV
1	Larger diameter of the elliptical section	2a	mm	Input	38.00	251.29	570.00	139.52	0.56
2	Smaller diameter of the elliptical section	2b	mm	Input	38.00	163.13	570.00	110.28	0.68
3	Thickness of steel tube	t	mm	Input	0.90	6.47	26.00	5.02	0.78
4	Yield strength of steel	$f_{\rm v}$	MPa	Input	182.90	379.03	834.00	81.39	0.21
5	Concrete compressive strength	$f_c$	MPa	Input	13.00	56.31	120.00	25.90	0.46
6	Measure of relative slenderness	2b/L	_	Input	0.02	0.25	0.71	0.15	0.63
7	Axial Load-Carrying Capacity	$N_u$	kN	Output	107.60	4946.87	37494.00	7369.36	1.49

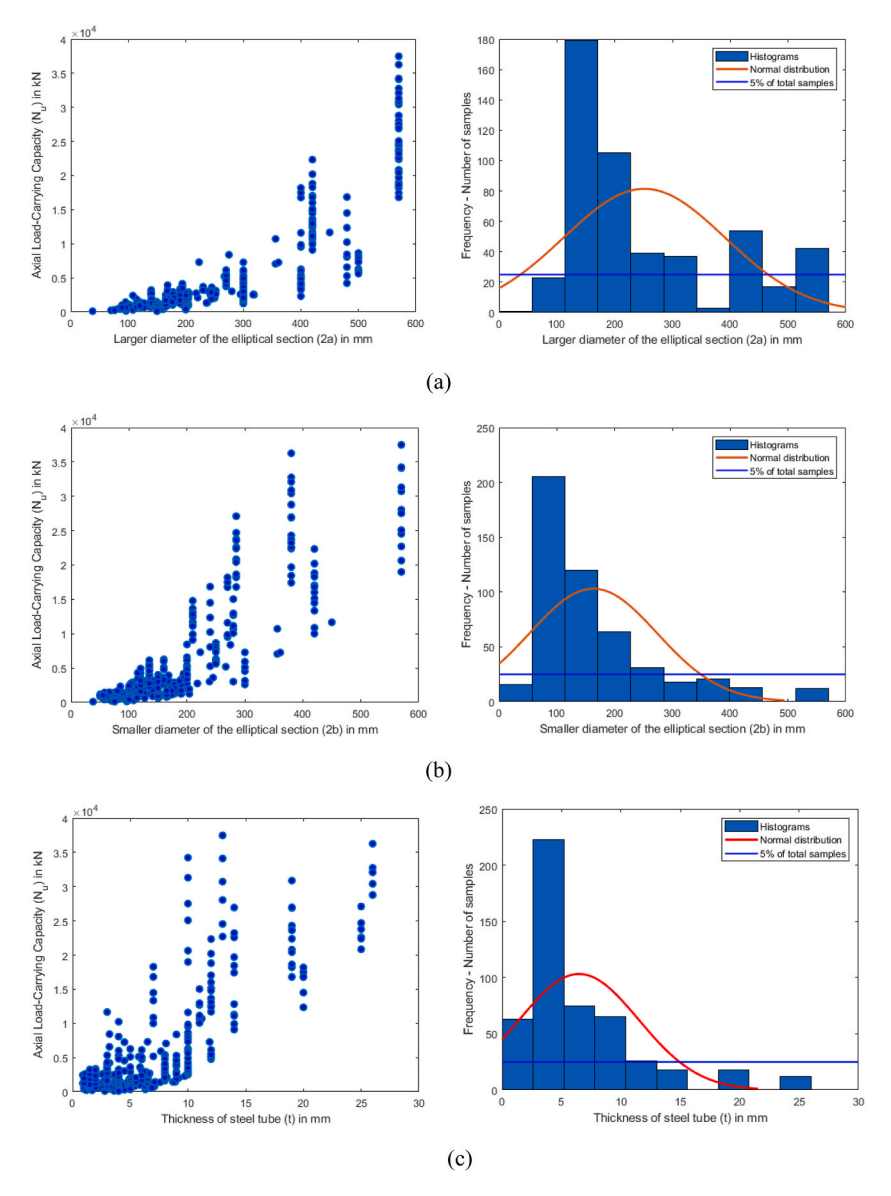


Fig. 1. Histograms of parameters used for the prediction of Axial Load-Carrying Capacity  $(N_u)$ : (a) Axial Load-Carrying Capacity  $(N_u)$  vs Larger Diameter of the elliptical section (2a), (b) Axial Load-Carrying Capacity  $(N_u)$  vs Smaller Diameter of the elliptical section (2b), (c) Axial Load-Carrying Capacity  $(N_u)$  vs Thickness of steel tube (t), (d) Axial Load-Carrying Capacity  $(N_u)$  vs Yield strength of steel  $(f_y)$ , (e) Axial Load-Carrying Capacity  $(N_u)$  vs Concrete compressive strength  $(f_c)$ , (f) Axial Load-Carrying Capacity  $(N_u)$  vs measure of relative slenderness (2b/L).

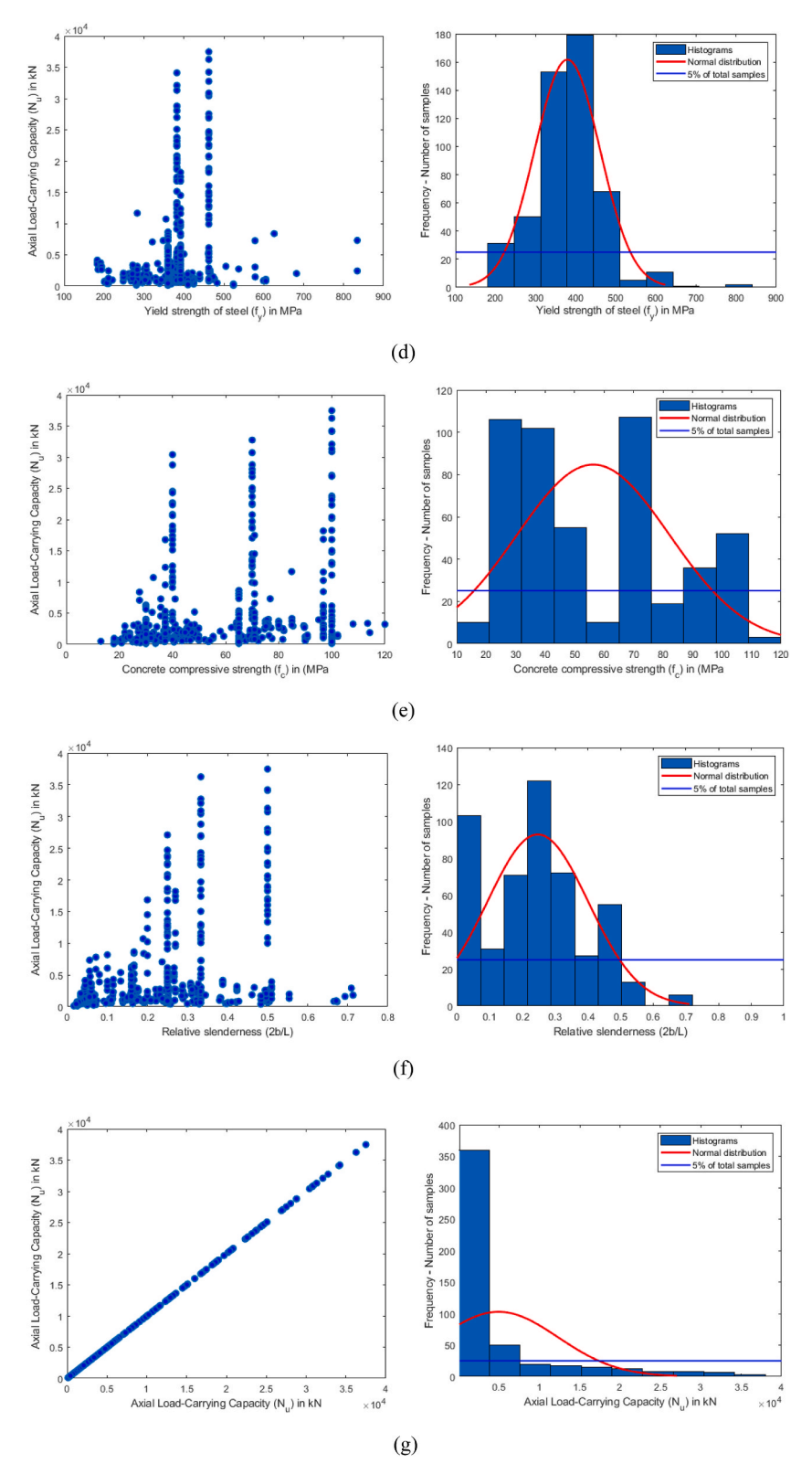


Fig. 1. (continued).

**Table 4**Pearson Correlation Coefficients of input and output parameters.

Variable	Symbol	2 <i>a</i>	2b	t	fy	$f_c$	2b/L	$N_u$
Larger diameter of the elliptical section	2a	1.00						
Smaller diameter of the elliptical section	2b	0.82	1.00					
Thickness of steel tube	t	0.74	0.59	1.00				
Yield strength of steel	$f_{y}$	0.13	0.08	0.29	1.00			
Concrete compressive strength	$f_c$	0.26	0.14	0.21	0.06	1.00		
Measure of relative slenderness	2b/L	0.13	0.45	0.09	0.17	0.09	1.00	
Axial Load-Carrying Capacity	$N_u$	0.87	0.87	0.82	0.21	0.30	0.31	1.00

columns both at cross-sectional and member level. The design of the cross-sectional and member compression capacity is often treated separately in codes, as shown in Section 2.1. To account for the influence of member's slenderness, the ratio of the member's length and the smaller (minor axis) diameter has been included as one of the parameters (2b/L), as shown in Fig. 1(f). Fig. 1(g) shows the range of axial load-carrying capacity values of the applied dataset.

Both Table 3 and Fig. 1 are capital as they define the validity range of the soft computing model that will be trained and developed for estimating axial load-carrying capacity. This is a crucial issue and will be further discussed in a subsequent section titled "Limitations and Future Research."

In addition, Pearson Correlation Coefficients between each pair of variables in the dataset are given in Table 4. As shown in Table 4, the diameters in both axes are strongly correlated (0.82). Next, Pearson Correlation Coefficient between length of the major axis and thickness of steel tube is 0.74. Besides, the max value of Pearson Correlation Coefficient is observed between length of the major axis and axial load-carrying capacity (0.87). The axial load-carrying capacity is also highly correlated to thickness of steel tube (0.82). Thus, it can be stated that there are several initial statistical correlations exist within the input space.

## 3.2. Methodology

This section provides a detailed and in-depth description of the methodology followed to identify the optimal soft computing model for estimating the axial load-carrying capacity of concrete-filled steel tubes with elliptical hollow sections. The key steps of the methodology are as follows.

- I. Data Splitting and Normalization: The database, consisting of 500 datasets, was divided into two subsets: 400 datasets (80 %) were used for model training, and the remaining 100 datasets (20 %) were used for model testing. It is important to note how the data was split. The most significant disadvantage of splitting data into a single training set and a single test set is the possibility that the test set may not follow the same class distribution as the overall data, and some numerical features may not have the same distribution in the training and test sets. Considering this, the 80/20 split of the database was performed using the k-fold cross-validation technique with 5 folds [57]. This data splitting process was carried out with normalization of the data using six different classical normalization methods.
- II. Simulation Method: To estimate the axial load-carryingcapacity of the composite columns, Back Propagation Neural Networks (BPNN) models were utilized and trained using (i) four different optimization algorithms: Levenberg-Marquardt (LM) algorithm [58], Broyden–Fletcher–Goldfarb–Shanno (BFGS) algorithm [59], Particle Swarm Optimization (PSO) algorithm [60], and the Imperialist Competitive Algorithm (ICA) [61], (ii) architectures with 1 hidden layer, (iii) architectures with 1–30 neurons per hidden layer, with a step of 1, as opposed to using semi-empirical formulas that have been proposed for determining the number of neurons and are commonly used by most researchers [62], and (iv) 12 different transfer functions, leading to 144 (12^2) different combinations for architectures with 1 hidden layer. It is worth noting that most researchers use at most four transfer functions, which makes the evaluation of optimization algorithms incomplete and often leads to incorrect conclusions. This will be discussed and demonstrated in the next section, where the results of this study will be presented. For brevity, the full set of parameters used is thoroughly discussed in the document titled *Parameters of ANNs*, which has been appended as supplementary material to this manuscript.
- III. Optimal Forecasting Model: The combination of the above parameters resulted in the training and development of many different architectures. All these architectures were evaluated and ranked based on their performance, which was determined using classic and widely accepted performance indices, such as the root mean square error (RMSE), the mean absolute percentage error (MAPE), the values account for (VAF), and the correlation coefficient (R) [63]. Additionally, the a20-index, recently proposed [64–66], and widely adopted, was applied for the assessment of the developed models. The a20-index is defined by:

$$a20-index = \frac{m20}{M}$$
 (x)

where M is the number of dataset samples and m20 is the number of samples with a value of (experimental value)/(predicted value) ratio between 0.80 and 1.20. The adoption of the a20-index within the  $\pm 20$  % range is justified by the high coefficient of variation observed in the results of compression tests of ECFST specimens. The a20-index ranges from 0 to 1, with higher values indicating better

performance, and for an ideal predictive model, the a20-index is expected to be close to 1.

- IV. Assessment of the Contribution of Each Feature to the Prediction: One of the primary goals of this study is to evaluate the parameters involved in the problem based on their influence on the axial load-carrying capacity of concrete-filled steel tubes with elliptical hollow sections. For this purpose, using the optimal developed model from the previous step and the SHapley Additive exPlanations (SHAP) method proposed by Ref. [67,68], the importance of each input parameter on the output parameter is determined and ranked according to their influence from the most to the least significant.
- V. Mapping and Revealing the Nature of axial load-carrying capacity of elliptical concrete-filled steel tubular columns: In this final step of the methodology, using the optimal developed model, a set of graphs is constructed.

### 4. Results and discussion

## 4.1. Training and development of ANN models

Following the methodology detailed in the previous section, BPNN (Back Propagation Neural Network) models were designed and trained for the estimation of the axial load-carrying capacity of ECFST columns. Specifically, using the parameters outlined in the supplementary materials titled *Parameters of ANNs*, a total of 1,555,200 different neural network architectures were trained and developed.

The top 20 architectures, based on the RMSE (Root Mean Square Error) performance index for Testing Datasets, were identified for each of the four optimization algorithms. Additionally, the top 20 architectures across all four optimization algorithms are provided in the Excel file titled *Top* 20 ANN *Architectures*, which is appended as supplementary material to this work. Furthermore, Table 5 presents the optimal architecture for each of the four optimization algorithms.

Based on the results presented in the Top 20 architectures for each one of the four optimization algorithms, the following key findings are revealed during the modelling of axial load-carrying capacity of ECFST columns.

• Optimization Algorithms: The best performing optimization algorithm was the Levenberg-Marquardt algorithm, followed by the Broyden–Fletcher–Goldfarb–Shanno (BFGS) quasi-Newton algorithm, the Particle Swarm Optimization (PSO) algorithm, and the Imperialist Competitive Algorithm (ICA),

Table 5
Best ANN architectures for each one optimization algorithm based on RMSE performance index for Testing Datasets.

Ranking	Model	Architecture	Performa	nce Indices					Comments
			Testing I	Datasets	Training	Datasets	All Datas	sets	
			R	RMSE (MPa)	R	RMSE (MPa)	R	R RMSE (MPa)	
1	ANN- LM	4-27-1	0.9994	236.0444	0.9999	77.5124	0.9999	126.2930	Normalization Technique: Minmax [0.00, 0.50]; Cost Function: MSE Transfer function at the hidden layer: radbas, while Transfer function at the output layer: tansig
2	ANN- BFGS	6-29-1	0.9990	312.5104	0.9999	180.3668	0.9994	258.2744	Normalization Technique: Z-score Cost Function: SSE Transfer function at the hidden layer: tansig, while Transfer function at the output layer: purelin
4	ANN- ICA	6-12-1	0.9952	776.3808	0.9951	851.1393	0.9951	836.8010	Normalization Technique: Minmax [0.00, 0.50]; Cost Function: MSE Transfer function at the hidden layer: tansig, while Transfer function at the output layer: purelin Population: 50 Empires: 6
3	ANN- PSO	6-12-1	0.9923	950.9982	0.9942	921.0663	0.9938	927.1401	Normalization Technique: Minmax [0.00, 0.50]; Cost Function: MSE Transfer function at the hidden layer: tansig, while Transfer function at the output layer: purelin Population: 70

ANN-LM: Artificial Neural Network optimized by Levenberg-Marquardt algorithm.

ANN-BFGS: Artificial Neural Network optimized by Broyden-Fletcher-Goldfarb-Shanno quasi-Newton algorithm.

ANN-PSO: Artificial Neural Network optimized by Particle swarm optimization algorithm.

ANN-ICA: Artificial Neural Network optimized by Imperialist Competitive Algorithm.

- Transfer Functions: The superior transfer function for the hidden layer was found to be the Radial Basis (RB) function, followed by the Softmax (SM) transfer function. It is worth noting that these two transfer functions are rarely used by researchers. For the output layer, the dominant transfer functions were, in order, the Log-sigmoid (LS) transfer function, the Radial Basis (RB) transfer function, the Symmetric Saturating Linear (SL) transfer function, and the Linear (Li) transfer function.
- Normalization Techniques: The Minmax normalization technique in the range [0.00, 1.00] was found to be the most effective for data normalization,
- Neurons Per Layer: The optimal number of neurons per layer varied significantly depending on the optimization algorithm used.
   This finding suggests that the semi-empirical formulas commonly proposed in the literature for determining the number of neurons are not reliable.

These results underscore the complexity and specificity required in optimizing ANN models for predicting the axial load-carrying capacity of composite columns, highlighting the importance of careful selection of network architecture, transfer functions, and normalization techniques.

## 4.2. Optimal ANN model

The architecture of the optimum ANN-LM 6-27-1 model is shown in Fig. 2 and its prediction performance is indicated in Table 6. Fig. 2 also presents the optimum activation function for each layer and the optimum number of neurons in the hidden layer. As shown in Table 6, prediction performances a20-index, R, RMSE, MAPE and VAF of ANN-LM 4-27-1 are 0.96, 0.9999, 77.5124, 0.0482 and 99.9893, respectively, using training dataset, 0.8700, 0.9994, 236.0444, 0.0845 and 99.8795 using testing dataset. For all data points, a20-index, R, RMSE, MAPE and VAF are 0.9420, 0.9999, 126.2930, 0.0555 and 99.9706, respectively. It is seen that the prediction performance of the optimum ANN-LM 6-27-1 model outperforms existing models in the literature as shown in Table 1 for elliptical section.

Fig. 3 presents the experimental/FE and predicted (ANN-LM 6-27-1 model) load values for both training and testing data. The values align closely along the diagonal, indicating a highly accurate estimation. Fig. 4 presents the ratios of experimental to predicted values plotted versus 2b/L, demonstrating an acceptable scatter across the entire slenderness range and indicating good accuracy for load predictions for both higher and lower slenderness values.

### 4.3. ANN-based closed Form equation and GUI for the estimation of the axial load-carrying capacity of ECFST columns

In this section, we deduce an empirical equation for the prediction of axial load-carrying capacity of elliptical CFST members, based on the optimum ANN-LM 6-27-1 developed previously. The proposed equation is provided in matrix form below:

$$N_u = 74773 \times tansig([L_W] \times [radbas([I_W] \times [IP] + [b_i])] + [b_0]) + 107.60$$
(11)

where [IP] is a  $6 \times 1$  vector with the normalized values of the four input parameters given by:

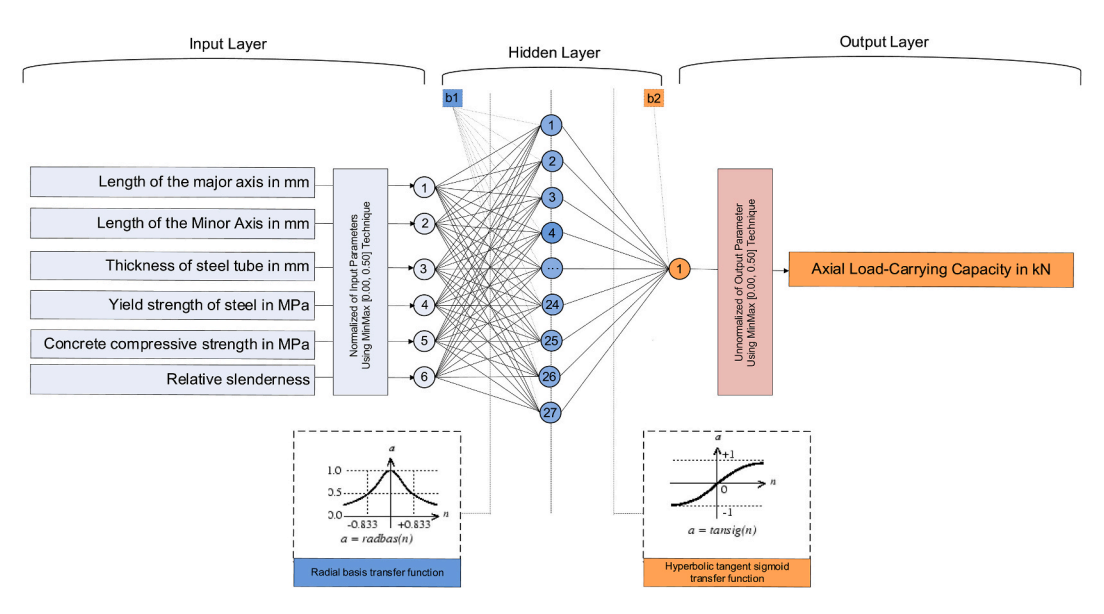


Fig. 2. Architecture of the optimal ANN-LM 6-27-1 model.

Table 6 Summary of prediction capability of the optimum ANN-LM 6-27-1 model.

Model	Datasets	Performance Indi	Performance Indices							
		a20-index	a20-index R		MAPE	VAF (%)				
ANN-LM4-9-1	Training Testing All	0.9600 0.8700 0.9420	0.9999 0.9994 0.9999	77.5124 236.0444 126.2930	0.0482 0.0845 0.0555	99.9893 99.8795 99.9706				

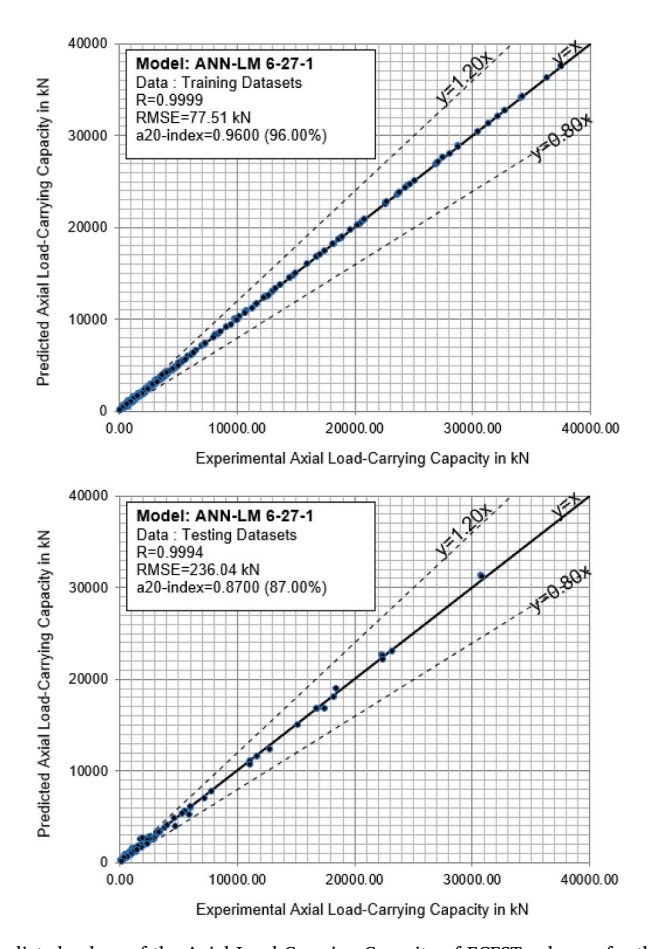


Fig. 3. Experimental ('true') vs Predicted values of the Axial Load-Carrying Capacity of ECFST columns for the developed and proposed optimal ANN-LM 6-27-1 model.

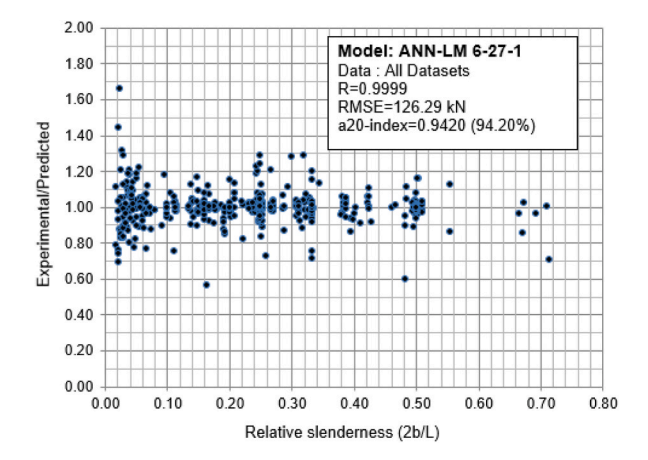


Fig. 4. Experimental ('true') to Predicted values of the Axial Load-Carrying Capacity of ECFST columns vs values of the measure of relative slenderness for the developed and proposed optimal ANN-LM 6-27-1 model.

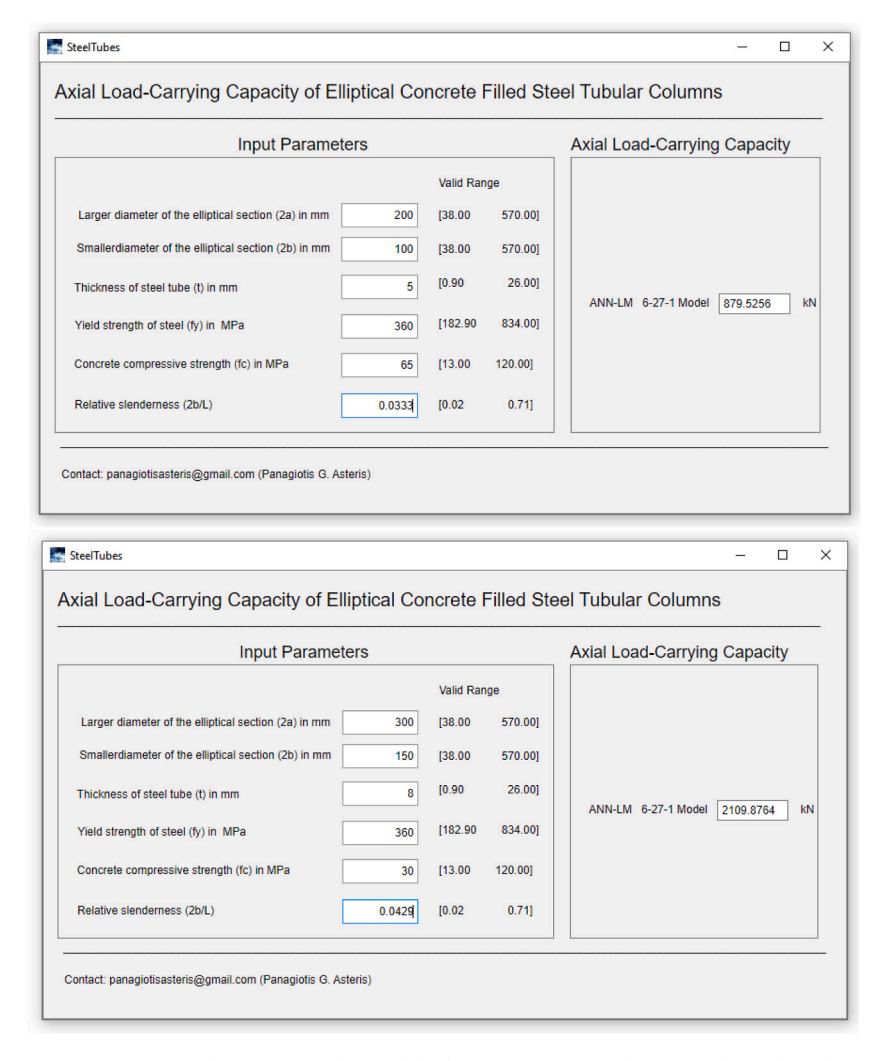


Fig. 5. Graphical User Interface (GUI) for the estimation the axial load-carrying capacity of ECFST columns based on optimal ANN-LM 6-27-1 model.

$$[IP] = \begin{bmatrix} \frac{2a - 38}{570} \\ \frac{2b - 38}{570} \\ \frac{t - 0.90}{26} \\ \frac{f_y - 182.90}{834.00} \\ \frac{f_c - 13.00}{120.00} \\ \frac{(2b/L) - 0.02}{0.71} \end{bmatrix}$$

$$(12)$$

in this equation, tansig is the Hyperbolic tangent sigmoid transfer function, and radbas refers to the Radial Basis transfer function.  $[I_W]$  is a  $27 \times 6$  containing the weights of the hidden layer,  $[L_W]$  is a  $1 \times 27$  vector containing the weights of the output layer,  $[b_i]$  is a  $27 \times 1$  vector containing the bias values of the hidden layer, and  $[b_0]$  is a  $1 \times 1$  vector containing the bias values of the output layer. All these matrices are provided as supplementary materials in the excel file titled *Final values of weights and biases*.

It should be noted that the implementation of the above empirical equations in a computer program requires only basic algebraic and matrix operations, making it computationally efficient and accessible for practical use. To facilitate the operation, a GUI has been developed and shown below (Fig. 5). This GUI provides an intuitive and user-friendly environment for applying Eq. (x) without retraining the machine learning models. It is worth noticing that Eq. (x) only valid for the range of input variables shown in the GUI. As shown in Fig. 5, the developed GUI provides clear input fields (e.g., material properties and geometric parameters) and real-time output (e.g., predicted load capacity), enabling designers to quickly test and verify design options. In general, the GUI for strength prediction of structural members can be integrated into the interface of widely used structural analysis and design tools, becoming part of the standard modelling process. Alternatively, it can be deployed independently as a standalone application or as a plug-in within existing design suites, offering dedicated functionality (i.e., ECFST column strength prediction) without disrupting established workflows.

## 4.4. Comparison of the developed models and available proposals in the literature

Table 7 presents a comparison of the considered design prediction models based on key performance indices, including the a20-index, R, RMSE, MAPE, and VAF. The model proposed herein achieves the highest a20-index value of 0.9420, demonstrating superior accuracy and consistency in strength predictions. Similar observations are also made based on the Coefficient of Determination, where most models demonstrate good correlation values, with our proposed model achieving the highest value of 0.9999. This model also shows the lowest RMSE (126.293 kN) and MAPE (0.0555), further reinforcing its accuracy. EC4 using the confinement equations for circular hollow sections also achieves a high a20-index values of 0.8560, reflecting good accuracy of the strength prediction. A lower a20-index value (0.7100) is obtained, using the generic formula of Eurocode for composite cross-sections. The proposals by Ref. [5,13] also demonstrate good accuracy. Both approaches combine EC4 with the equivalent diameters for the ellipse, achieving R values of 0.9888 and 0.9895, respectively. However, using the [12] equation of the equivalent dimeter leads to a higher a20-index value. Despite the Chinese model being the only one that explicitly considers the elliptical section, it is still not the best design model. This can be attributed to the fact that the model was developed primarily using numerical data, as stated by Ref. [13], underscoring the need for more extensive experimental validation. American code has led to the lowers R value, whilst the model proposed by Ref. [2] for stub columns only demonstrates lower a20-index values (0.5960), and with higher error RMSE values, indicating less accurate prediction. These metrics highlight the advantages of the proposed model, in achieving both design accuracy and consistency.

**Table 7**Summary of prediction capability of the developed optimal model against proposals in literature, based on a20-index and testing datasets.

Source	Article's reference Section					
		a20-index	R	RMSE (kN)	MAPE	VAF
This article ANN-LM 6-27-1	Section 4.2	0.9420	0.9999	126.2930	0.0555	99.9706
EC4	Section 2.1.1.1	0.7100	0.9924	1924.5085	0.3032	96.8125
EC4 - confinement for circular	Section 2.1.1.2	0.8560	0.9949	1093.6118	0.1931	98.7531
[5]	Section 2.1.1.3	0.7900	0.9888	1510.3143	0.2392	97.5626
[13]	Section 2.1.1.4	0.6640	0.9895	2187.8565	0.2820	95.5246
[15]	Section 2.1.2	0.6020	0.8954	4369.0852	0.3693	79.8285
Chinese GB50936 [16]	Section 2.1.3	0.6760	0.9694	2394.7894	0.4187	93.9432
[2]	Section 2.1.4	0.5960	0.9943	2173.0412	0.3055	96.2231

## 4.5. Assessment of the parameters affecting the axial load-carrying capacity of ECFST columns

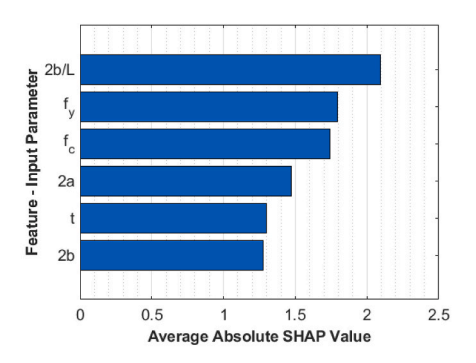
Aiming to reveal the nature of steel tubes, this subsection seeks to evaluate the parameters that influence the value of axial load-carrying capacity of concrete-filled steel tubes with elliptical hollow sections and to rank them based on their impact. For this purpose, the optimal developed ANN-LM 6-27-1 model and the SHapley Additive exPlanations (SHAP) method, recently proposed [67,68], are used to determine the significance of each input parameter on the output parameter. These parameters are then ranked from the most to the least influential. SHAP analysis can be used to interpret machine learning models by assigning each input feature an importance value for a particular prediction, thus explaining how much each feature contributes, positively or negatively, to the model's output. This helps to understand the model's decision-making process and identify key influencing variables.

In Fig. 6, the parameters are presented in descending order of their influence, from the most to the least significant. Specifically, the figure shows the average SHAP values for each of the four input parameters (Fig. 6(a)) and the SHAP values for each individual sample (dataset) (Fig. 6(b)). Based on these figures, it is evident that the most important parameter affecting the axial load-carrying capacity is the measure of relative slenderness (2b/L) (SHAP value: 2.09) followed in order by the yield strength of steel ( $f_y$ ), (SHAP value: 1.79) the concrete compressive strength ( $f_c$ ) (SHAP value: 1.73), the larger diameter of the elliptical section (2a), (SHAP value: 1.47) the thickness of the steel tube (t), (SHAP value: 1.30.) and last the smaller diameter of the elliptical section (2b) (SHAP value: 1.28)

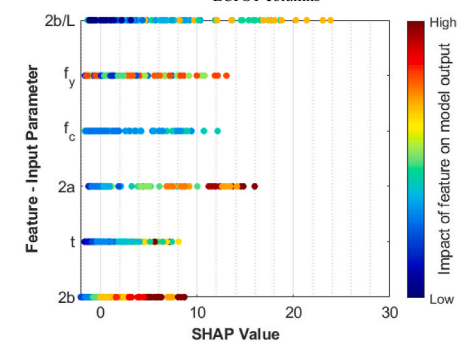
Despite the fact that this classification appears to be in agreement with the existing experimental knowledge—given that the primary parameter identified is the measure of relative slenderness (2b/L), followed by the yield strength of steel  $(f_y)$ —we must be particularly cautious, as this classification depends on how capable and reliable the database used for training the soft computing predictive model is.

In this direction, contrary to what is commonly followed in the literature, it was deemed appropriate to conduct a classification of parameters using the same method (SHapley Additive exPlanations) but selecting a different database. Specifically, a subset of the database was used, consisting of only 162 datasets corresponding to 'short' steel tube columns from the original database of 500 samples. The criterion for selecting these data was that the (2b/L) value had to be greater than 0.30. The results are illustrated in Fig. 7.

Based on these results, and as expected from the available experimental knowledge for short columns, the primary parameter influencing the axial load-carrying capacity is the yield strength of steel  $(f_y)$  (Fig. 6).



 Mean SHAP value of input parameters influencing the axial load-carrying capacity of ECFST columns



b) SHAP value for each one dataset of input parameters influencing the axial load-carrying capacity of ECFST columns

Fig. 6. Assessment of the parameters influencing the axial load-carrying capacity of ECFST columns based on optimal ANN-LM 6-27-1 model and using SHapley Additive exPlanations (SHAP) method.

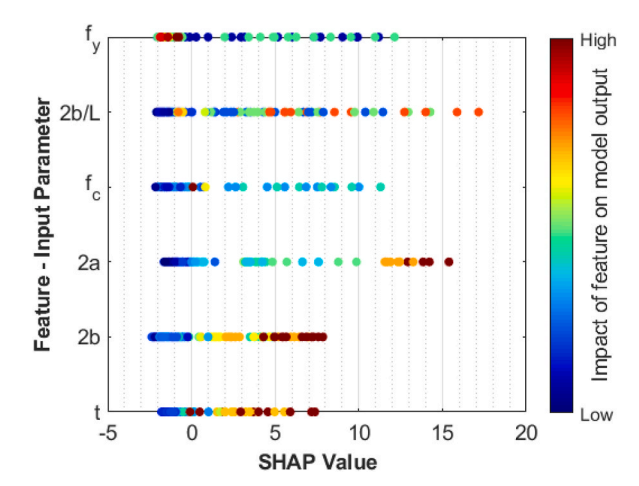


Fig. 7. Assessment of the parameters influencing the axial load-carrying capacity of ECFST columns based on optimal ANN-LM 6-27-1 model and using SHapley Additive exPlanations (SHAP) method and using data only from 'short' steel tubes columns (measure of relative slenderness (2b/L) greater than 0.30).

## 4.6. Mapping and revealing the nature of steel tubes columns with elliptical hollow sections

In this section, using the proposed optimal ANN-LM 6-27-1 model, an attempt will be made to map and reveal the complex nature of steel tubes through the production of a set of graphs. These graphs will also demonstrate that the well-known and frequently encountered problem of overfitting did not occur during the model's training. Specifically, Fig. 8 presents the case of an ECFST column with an elliptical cross-section of  $150 \times 300$  mm, a steel tube with thickness of 6, 8, 10, 12 mm, see Fig. 9(a–d), respectively, and concrete infill with compressive strength equal to 20 MPa. The strength prediction trend curves of the same column are shown in Fig. 9, but with an alternative axis for the axial load-carrying capacity and the effect of the member slenderness.

Based on these mappings, the following points can be made.

- The smoothness of the contours confirms that the proposed computational methodology avoids the overfitting of data, a common issue in the development of prognostic soft computing models. In cases of overfitting, the model may appear to fit very closely to the experimental data used for its training; however, for slightly perturbed data ranges, the predictions become significantly worse,
- Fig. 8 shows the anticipated trend of increasing axial load-carrying capacity for increasing (2b/L) (i.e. for decreasing member slenderness) and for increasing steel thickness. The effect of the steel grade is also evident, whilst the formation of a strength plateau for increasing 2b/L, which is more evident in Fig. 8(c) and (d) that correspond to steel tubes of larger thickness, reflects that the capacity is governed by the plastic compression resistance for columns with smaller member slenderness values.
- The influence of both the relative member slenderness and steel grade is also clearly evident in Fig. 9. It can also be observed that the lower curves of 2b/L (representing slender columns) are relatively close one another, particularly for higher steel grades, where their capacity is governed by flexural buckling.

These graphs are particularly useful for practicing engineers in the design of reliable steel tubes structures. They are also valuable for supporting academic lectures and related coursework.

## 5. Limitations and future research

Despite the promising accuracy and practical applicability of the ANN-LM 6-27-1 model for predicting the axial load-carrying capacity of elliptical CFSTs, several limitations remain.

- First of all, the model was trained within a specific range of geometric and material properties. Predictions, involving extrapolation (i.e., estimating values beyond the range of the training data for out-of-range values) may not be reliable without additional validation. Future studies could conduct targeted experiments on underrepresented parameters-covering a wider range of material strengths, section dimensions, and loading conditions. The histogram parameters presented earlier in Fig. 1 highlight gaps in the literature that should be addressed through targeted experimental work. For example, it can be seen that there are limited studies with ECFSTs using higher strength steels. These additional experimental studies can provide high-quality training and validation data, enhancing the model's to generalisability and robustness.
- This study was based on available data from literature. Given the limited availability of data on elliptical hollow sections, the dataset was expanded to include concrete-filled steel hollow sections with both elliptical and circular cross-sections, treating circular sections as a special case of elliptical sections with an aspect ratio a/b = 1 to ensure a sufficiently large database. This approach enabled the creation of a larger, more comprehensive database, which was deemed necessary and crucial for developing a

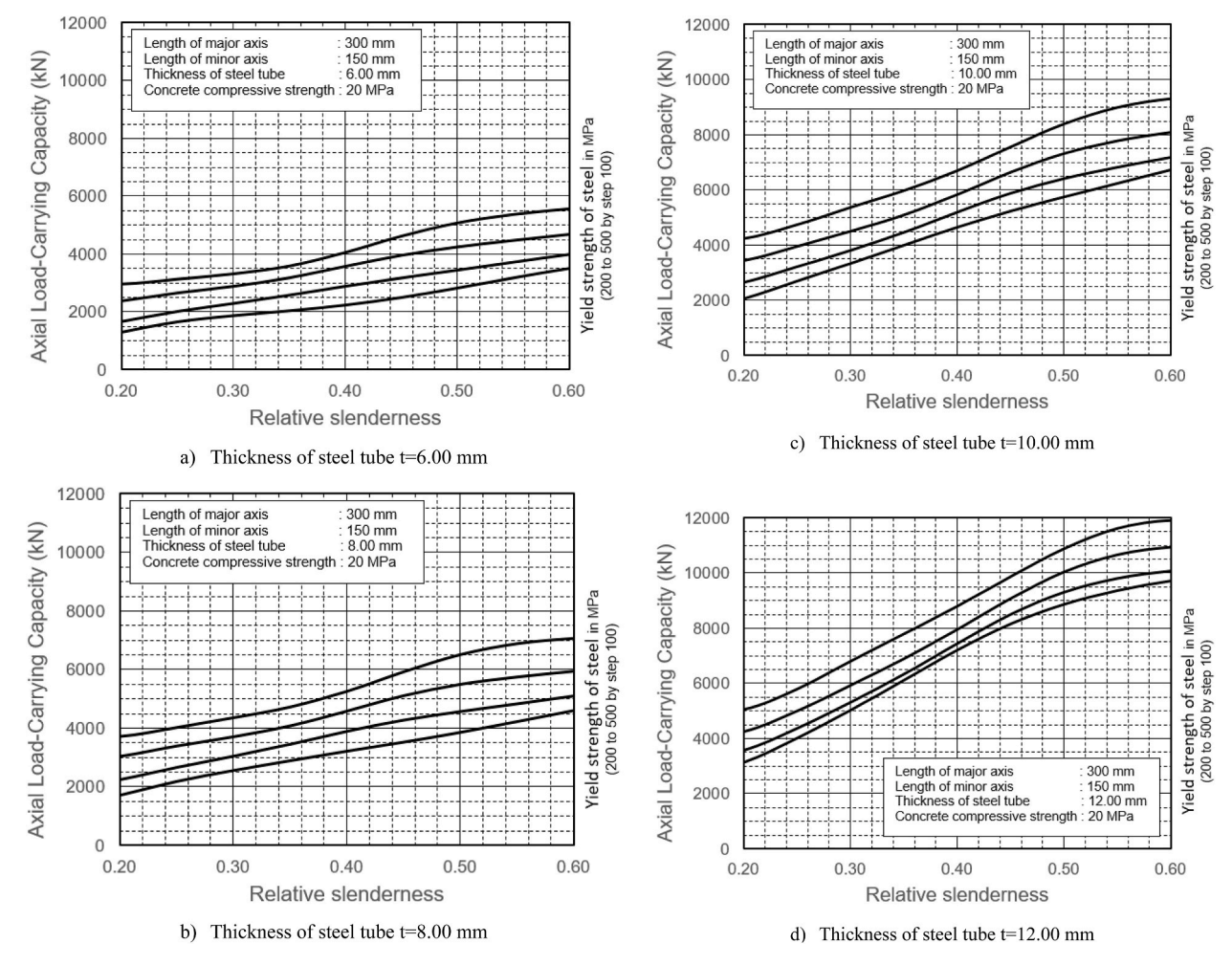


Fig. 8. Axial load-carrying capacity vs measure relative slenderness (2b/L) of steel tubes using the optimal ANN-LM 6-27-1 model.

reliable computational intelligence model. Although the underlying confinement mechanics between the circular and elliptical shapes differ, this study aimed to provide a simplification and focus on developing a generalized predictive model, without explicitly including the cross-sectional aspect ratio as an input parameter. Future investigations could include the cross-sectional aspect ratio a/b parameter as input variable, enabling the model to capture the cross-sectional shape effects more accurately.

- The current study focuses on axial loading conditions. Future research should consider various load conditions and design scenarios [69–71], such as eccentric loading, seismic behaviour, and fire resistance to develop more comprehensive predictive models. Alongside this, it is recommended to conduct sensitivity analyses for each load scenario to identify which variables most significantly influence the model's predictions and how. Additionally, further research into the underlying constitutive laws [72] is essential to deepen understanding and improve model accuracy.
- Last but not least, the current study did not evaluate the uncertainty existing in the input space and how it propagates to the output
  response. Thus, probabilistic and reliability-based approaches [73] should also be implemented to assess the confidence intervals of
  predictions.

## 6. Conclusions

This research study presented a robust computational model capable of accurately estimating the axial load-carrying capacity of elliptical concrete-filled steel tubular (EFCST) columns. The following conclusions summarise the main findings of the study.

 The experimental database included 500 data points covering a wide range of geometry and material parameters, including both stub and slender columns (namely 367 stub columns and 133 slender columns), which are often treated separately in design codes for composite structures.

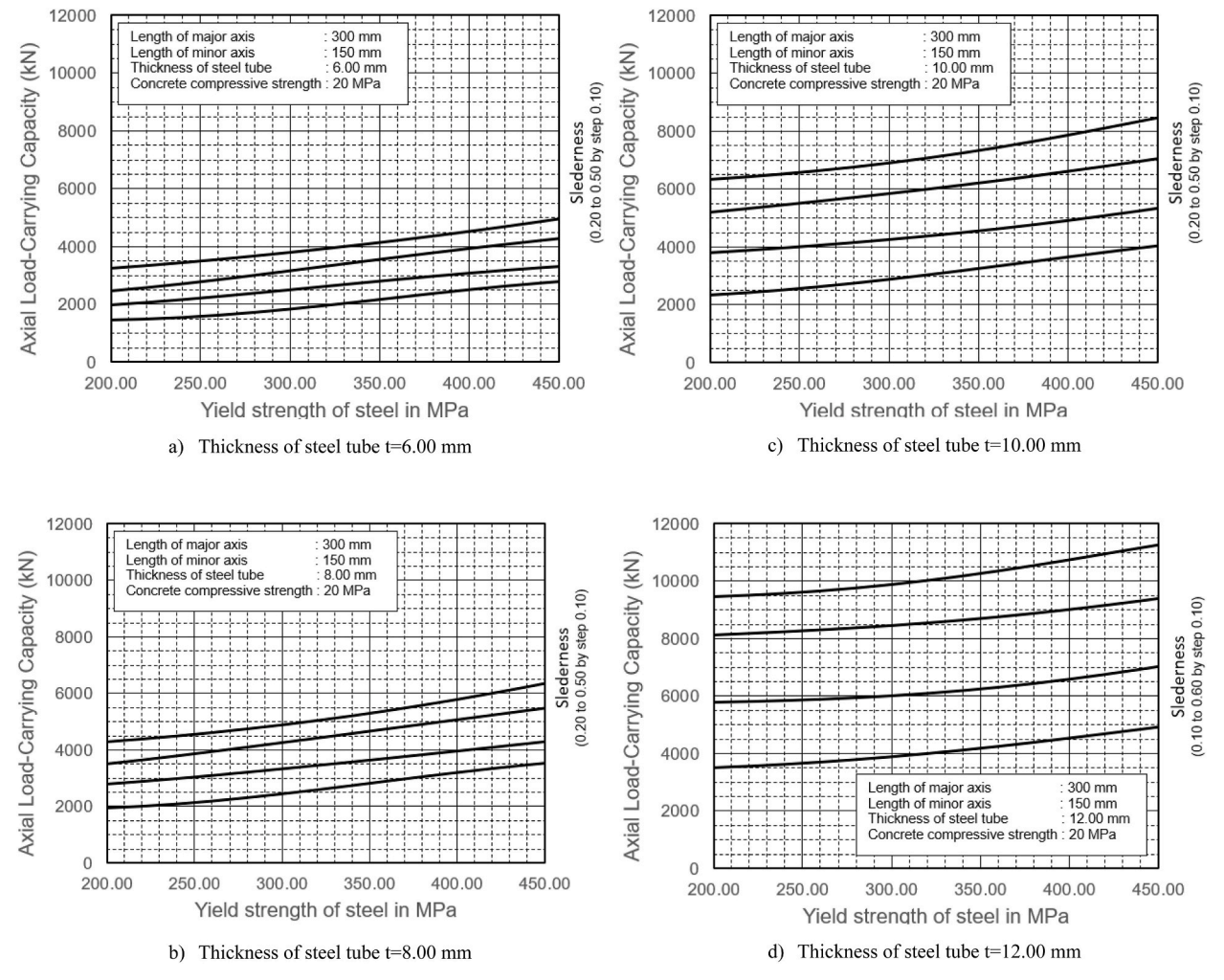


Fig. 9. Axial load-carrying capacity vs Yield strength of steel tubes using the optimal ANN-LM 6-27-1 model.

- An optimization procedure was carried out to develop the optimum proposed algorithm. A total of 1,555,200 neural network
  architectures were trained and developed. For each of the four optimization algorithms considered, the top 20 architectures were
  identified based on their performance on the testing datasets.
- The architecture of the optimum ANN-LM 6-27-1 model has been presented in detail. The model achieved a-20 index value of 0.9999 and R<sup>2</sup> value of training and testing equal to 0.9999 and 0.9994, respectively, demonstrating exceptional prediction accuracy.
- A SHAP analysis was performed for the developed model, revealing that the most critical parameter for the entire dataset was the measure of relative slenderness (2 b/L) (SHAP value: 2.09).
- An assessment of design codes is also presented, highlighting the superiority of the proposed model in terms of design accuracy and consistency. The proposed model has achieved the highest a20-index value of 0.9420 and R equal to 0.9999.
- Good design predictions have also been achieved by EC4 using the conferment design for circular hollow sections (a20-index value of 0.8560 and R equal to 0.9949), or in combination with the equivalent diameter for the elliptical section proposed by Gardner and Chan [12] (a20-index value of 0.7900 and R equal to 0.9888)
- Based on the proposed model ANN-LM 6-27-1, an empirical formula together with a graphical interface has been developed and is
  provided freely for researchers and engineers.

The findings of this study have the potential to simplify the design procedure for ECFST columns which is currently not adequately addressed by the design codes. The proposed optimum model leads to exceptionally accurate prediction of the axial load-carrying capacity of ECFST columns, whilst effectively accommodating the cases of high-strength steel, high-strength concrete, slender cross-sections and slender columns.

## CRediT authorship contribution statement

Panagiotis G. Asteris: Writing – review & editing, Writing – original draft, Supervision, Software, Methodology, Investigation, Conceptualization. Tryfon Sivenas: Writing – review & editing, Writing – original draft, Software, Methodology, Investigation, Formal analysis. Michaela Gkantou: Writing – review & editing, Writing – original draft, Visualization, Validation, Supervision, Methodology, Investigation, Formal analysis. Antonio Formisano: Writing – review & editing, Writing – original draft, Visualization, Validation, Methodology, Investigation. Tien-Thinh Le: Writing – review & editing, Writing – original draft, Visualization, Validation, Software, Methodology, Investigation, Formal analysis.

### Declaration of competing interest

The authors declare that they have no known competing financial interests or personal relationships that could have appeared to influence the work reported in this paper.

## Appendix A. Supplementary data

Supplementary data to this article can be found online at https://doi.org/10.1016/j.jobe.2025.113738.

## Data availability

Data will be made available on request.

#### References

- [1] D. Lam, L. Gardner, M. Burdett, Behaviour of axially loaded concrete filled stainless steel elliptical stub columns, Adv. Struct. Eng. 13 (3) (2010), https://doi.org/10.1260/1369-4332.13.3.493. Article 3.
- [2] K. Uenaka, Experimental study on concrete filled elliptical/oval steel tubular stub columns under compression, Thin-Walled Struct. 78 (2014) 131–137, https://doi.org/10.1016/j.tws.2014.01.023.
- [3] F. McCann, L. Gardner, W. Qiu, Experimental study of slender concrete-filled elliptical hollow section beam-columns, Journal of Constructional Steel Research 113 (2015) 185–194
- [4] H. Yang, F. Liu, T. Chan, W. Wang, Behaviours of concrete-filled cold-formed elliptical hollow section beam-columns with varying aspect ratios, Thin-Walled Struct. 120 (2017) 9–28, https://doi.org/10.1016/j.tws.2017.08.018.
- [5] N. Jamaluddin, D. Lam, X.H. Dai, J. Ye, An experimental study on elliptical concrete filled columns under axial compression, J. Constr. Steel Res. 87 (2013) 6–16, https://doi.org/10.1016/j.jcsr.2013.04.002.
- [6] D. Li, J.-H. Nie, H. Wang, T. Yu, K.S.C. Kuang, Path planning and topology-aided acoustic emission damage localization in high-strength bolt connections of bridges, Eng. Struct. 332 (2025) 120103, https://doi.org/10.1016/j.engstruct.2025.120103.
- [7] K. Wang, J. Cao, J. Ye, Z. Qiu, X. Wang, Discrete element analysis of geosynthetic-reinforced pile-supported embankments, Constr. Build. Mater. 449 (2024) 138448, https://doi.org/10.1016/j.conbuildmat.2024.138448.
- [8] K. Wang, J. Ye, X. Wang, Z. Qiu, The soil-arching effect in pile-supported embankments: a review, Buildings 14 (1) (2024), https://doi.org/10.3390/buildings14010126. Article 1.
- [9] Y. Niu, W. Wang, Y. Su, F. Jia, X. Long, Plastic damage prediction of concrete under compression based on deep learning, Acta Mech. 235 (1) (2024) 255–266, https://doi.org/10.1007/s00707-023-03743-8.
- [10] Eurocode 4, Eurocode 4: Design of Composite Steel and Concrete Structures. Part 1.1, General Rules and Rules for Buildings, European Committee for Standardization, British Standards Institution, 2004.
- [11] Eurocode 3, Eurocode 3: Design of Steel Structures Part 1–1: General Rules and Rules for Buildings, European Committee for Standardization, British Standards Institution, 2005.
- [12] L. Gardner, T.M. Chan, Cross-section classification of elliptical hollow sections, Steel Compos. Struct. 7 (3) (2007). Article 3.
- [13] F. Liu, Y. Wang, T. Chan, Behaviour of concrete-filled cold-formed elliptical hollow sections with varying aspect ratios, Thin-Walled Struct. 110 (2017) 47–61, https://doi.org/10.1016/j.tws.2016.10.013.
- [14] A.M. Ruiz-Teran, L. Gardner, Elastic buckling of elliptical tubes, Thin-Walled Struct. 46 (11) (2008) 1304–1318, https://doi.org/10.1016/j.tws.2008.01.036.
- [15] AISC 360-10, Specification for Structural Steel Buildings ANSI/AISC 360-10, American Institute of Steel Construction, 2010.
- [16] GB50936, Technical Code for Concrete Filled Steel Tubular Structures, Ministry of Housing and Urban-Rural Development of the People's Republic of China, 2014.
- [17] P.G. Asteris, M.E. Lemonis, T.-T. Le, K.D. Tsavdaridis, Evaluation of the ultimate eccentric load of rectangular CFSTs using advanced neural network modeling, Eng. Struct. 248 (2021) 113297, https://doi.org/10.1016/j.engstruct.2021.113297.
- [18] M. Ahmadi, H. Naderpour, A. Kheyroddin, ANN model for predicting the compressive strength of circular steel-confined concrete, Int. J. Civ. Eng. 15 (2) (2017), https://doi.org/10.1007/s40999-016-0096-0. Article 2.
- [19] P.G. Asteris, K.D. Tsavdaridis, M.E. Lemonis, F.P.V. Ferreira, T.-T. Le, C.J. Gantes, A. Formisano, Al-powered GUI for prediction of axial compression capacity in concrete-filled steel tube columns, Neural Comput. Appl. (2024), https://doi.org/10.1007/s00521-024-10405-w.
- [20] H. Thanh Duong, H. Chi Phan, T.-T. Le, N. Duc Bui, Optimization design of rectangular concrete-filled steel tube short columns with Balancing bomposite cotion optimization and data-driven model, Structures 28 (2020) 757–765, https://doi.org/10.1016/j.istruc.2020.09.013.
- [21] E.M. Güneyisi, A. Gültekin, K. Mermerdaş, Ultimate capacity prediction of axially loaded CFST short columns, Int. J. Steel Struct. 16 (1) (2016), https://doi.org/10.1007/s13296-016-3009-9. Article 1.
- [22] H.F. Isleem, T. Qiong, M.M. Alsaadawi, M.K. Elshaarawy, D.M. Mansour, F. Abdullah, A. Mandor, N.H. Sor, A. Jahami, Numerical and machine learning modeling of GFRP confined concrete-steel hollow elliptical columns, Sci. Rep. 14 (1) (2024) 18647, https://doi.org/10.1038/s41598-024-68360-4.
- [23] T.-T. Le, P.G. Asteris, M.E. Lemonis, Prediction of axial load capacity of rectangular concrete-filled steel tube columns using machine learning techniques, Eng. Comput. (2021), https://doi.org/10.1007/s00366-021-01461-0.

- [24] T.-T. Le, H. Chi Phan, H. Thanh Duong, M. Vuong Le, Optimal design of circular concrete-filled steel tubular columns based on a combination of artificial neural network, balancing composite motion Algorithm and a large experimental database, Expert Syst. Appl. (2023) 119940, https://doi.org/10.1016/j.
- [25] H.-B. Ly, B.T. Pham, L.M. Le, T.-T. Le, V.M. Le, P.G. Asteris, Estimation of axial load-carrying capacity of concrete-filled steel tubes using surrogate models, Neural Comput. Appl. (2020), https://doi.org/10.1007/s00521-020-05214-w.
- [26] J. Moon, J.J. Kim, T.-H. Lee, H.-E. Lee, Prediction of axial load capacity of stub circular concrete-filled steel tube using fuzzy logic, J. Constr. Steel Res. 101 (2014) 184–191, https://doi.org/10.1016/j.jcsr.2014.05.011.
- [27] H.S. Mohamed, T. Qiong, H.F. Isleem, R.K. Tipu, R.I. Shahin, S.A. Yehia, P. Jangir, Arpita, M. Khishe, Compressive behavior of elliptical concrete-filled steel tubular short columns using numerical investigation and machine learning techniques, Sci. Rep. 14 (1) (2024) 27007, https://doi.org/10.1038/s41598-024-77396-5
- [28] H.Q. Nguyen, H.-B. Ly, V.Q. Tran, T.-A. Nguyen, T.-T. Le, B.T. Pham, Optimization of artificial intelligence System by evolutionary slgorithm for prediction of axial capacity of rectangular concrete filled steel tubes under compression, Materials 13 (5) (2020), https://doi.org/10.3390/ma13051205. Article 5.
- [29] Y. Ren, H.F. Isleem, W.J.K. Almoghaye, A.K. Hamed, P. Jangir, Arpita, G.G. Tejani, A.E. Ezugwu, A.A. Soliman, Machine learning-based prediction of elliptical double steel columns under compression loading, J. Big Data 12 (1) (2025) 50, https://doi.org/10.1186/s40537-025-01081-1.
- [30] V.-L. Tran, D.-K. Thai, D.-D. Nguyen, Practical artificial neural network tool for predicting the axial compression capacity of circular concrete-filled steel tube columns with ultra-high-strength concrete, Thin-Walled Struct. 151 (2020) 106720, https://doi.org/10.1016/j.tws.2020.106720.
- [31] V.-L. Tran, S.-E. Kim, Efficiency of three advanced data-driven models for predicting axial compression capacity of CFDST columns, Thin-Walled Struct. 152 (2020) 106744, https://doi.org/10.1016/j.tws.2020.106744.
- [32] X.H. Dai, D. Lam, N. Jamaluddin, J. Ye, Numerical analysis of slender elliptical concrete filled columns under axial compression, Thin-Walled Struct. 77 (2014) 26–35, https://doi.org/10.1016/j.tws.2013.11.015.
- [33] Q.-X. Ren, L.-H. Han, D. Lam, W. Li, Tests on elliptical concrete filled steel tubular (CFST) beams and columns, J. Constr. Steel Res. 99 (2014) 149–160, https://doi.org/10.1016/j.jcsr.2014.03.010.
- [34] N. Jamaluddin, Behaviour of Elliptical concrete-filled Steel Tube (CFT) Columns Under Axial Compression Load, Phd, University of Leeds, 2011. http://etheses.whiterose.ac.uk/11322/.
- [35] H. Yang, D. Lam, L. Gardner, Testing and analysis of concrete-filled elliptical hollow sections, Eng. Struct. 30 (12) (2008), https://doi.org/10.1016/j.engstruct.2008.07.004. Article 12.
- [36] X.L. Zhao, J.A. Packer, Tests and design of concrete-filled elliptical hollow section stub columns, Thin-Walled Struct. 47 (6) (2009), https://doi.org/10.1016/j.tws.2008.11.004. Article 6.
- [37] S. De Nardin, A.L.H.C. El Debs, Axial load behaviour of concrete-filled steel tubular columns, J. Constr. Steel Res. 160 (1) (2007), https://doi.org/10.1680/stbu.2007.160.1.13. Article 1.
- [38] Y. Ye, L.-H. Han, T. Sheehan, Z.-X. Guo, Concrete-filled bimetallic tubes under axial compression: experimental investigation, Thin-Walled Struct. 108 (2016) 321–332, https://doi.org/10.1016/j.tws.2016.09.004.
- [39] M. Mahgub, A. Ashour, D. Lam, X. Dai, Tests of self-compacting concrete filled elliptical steel tube columns, Thin-Walled Struct. 110 (2017) 27–34, https://doi.org/10.1016/j.tws.2016.10.015.
- [40] T.-M. Chan, Y.-M. Huai, W. Wang, Experimental investigation on lightweight concrete-filled cold-formed elliptical hollow section stub columns, Proc. Inst. Civil Eng. Struct. Build. 115 (2015) 434–444, https://doi.org/10.1016/j.jcsr.2015.08.029.
- [41] L. He, Y. Zhao, S. Lin, Experimental study on axially compressed circular CFST columns with improved confinement effect, J. Constr. Steel Res. 140 (2018) 74–81. https://doi.org/10.1016/j.jcsr.2017.10.025.
- [42] S. Yi, B. Young, Experimental investigation of concrete-filled cold-formed steel elliptical stub columns, in: Tubular Structures XVI, Proceedings of the 16th International Symposium for Tubular Structures, 2017, pp. 109–115, https://doi.org/10.1201/9781351210843-14.
- [43] M.H. Lai, J.C.M. Ho, Confinement effect of ring-confined concrete-filled-steel-tube columns under uni-axial load, Eng. Struct. 67 (2014) 123–141, https://doi.org/10.1016/j.engstruct.2014.02.013.
- [44] M.H. Lai, J.C.M. Ho, Behaviour of uni-axially loaded concrete-filled-steel-tube columns confined by external rings, Struct. Des. Tall Special Build. 23 (6) (2014), https://doi.org/10.1002/tal.1046. Article 6.
- [45] C.S. Huang, Y.-K. Yeh, G.-Y. Liu, H.-T. Hu, K.C. Tsai, Y.T. Weng, S.H. Wang, M.-H. Wu, Axial load behavior of stiffened concrete-filled steel columns, J. Struct. Eng. 128 (9) (2002), https://doi.org/10.1061/(ASCE)0733-9445(2002)128:9(1222. Article 9.
- [46] Stephen P. Schneider, Axially loaded concrete-filled steel tubes, J. Struct. Eng. 124 (10) (1998), https://doi.org/10.1061/(ASCE)0733-9445(1998)124:10
- [47] J. Xiao, Y. Huang, J. Yang, Ch Zhang, Mechanical properties of confined recycled aggregate concrete under axial compression, Constr. Build. Mater. 26 (1) (2012). https://doi.org/10.1016/j.conbuildmat.2011.06.062. Article 1.
- [48] A.A. Khalaf, K.Z. Naser, F. Kamil, Predicting the ultimate strength of circular concrete filled steel tubular columns by using artificial neural networks, Int. J. Civ. Eng. Technol. 9 (7) (2018). Article 7.
- [49] M. Tomii, K. Yoshimura, Y. Morishita, Experimental studies on concrete-filled steel tubular stub columns under concentric loading, 718–741, https://cedb.asce.org/CEDBsearch/record.jpp?dockey=0026696, 1977.
- [50] F. Havashi, Study on Mechanical Behavior of Circular Confined Concrete Column Under Axial Compression, Kyushu University, 1990.
- [51] T. Sato, Study on Interaction Between Steel Tube and Concrete of Circular concrete-filled Steel Tubular Structure System, Osaka University, 1995.
- [52] S. Yi, M.-T. Chen, B. Young, Design of concrete-filled cold-formed steel elliptical stub columns, Eng. Struct. 276 (2023) 115269, https://doi.org/10.1016/j.engstruct.2022.115269.
- [53] T.-Y. Song, C.-L. Li, Z. Chen, X.-L. Liu, H. Zhou, Post-fire performance of axially-loaded elliptical concrete-filled steel tubular stub columns, Structures 50 (2023) 2004–2023, https://doi.org/10.1016/j.istruc.2023.02.116.
- [54] J. Liao, Y.-L. Li, Y. Ouyang, J.-J. Zeng, Axial compression tests on elliptical high strength steel tubes filled with self-compacting concrete of different mix proportions, J. Build. Eng. 40 (2021) 102678, https://doi.org/10.1016/j.jobe.2021.102678.
- [55] Y. Cai, W.-M. Quach, B. Young, Experimental and numerical investigation of concrete-filled hot-finished and cold-formed steel elliptical tubular stub columns, Thin-Walled Struct. 145 (2019) 106437, https://doi.org/10.1016/j.tws.2019.106437.
- [56] Y. Xu, J. Yao, X. Sun, Cold-formed elliptical concrete-filled steel tubular columns subjected to monotonic and cyclic axial compression, Adv. Struct. Eng. 23 (7) (2020), https://doi.org/10.1177/1369433219894242. Article 7.
- [57] N.F. Alkayem, L. Shen, A. Mayya, P.G. Asteris, R. Fu, G. Di Luzio, A. Strauss, M. Cao, Prediction of concrete and FRC properties at high temperature using machine and deep learning: a review of recent advances and future perspectives, J. Build. Eng. 83 (2024) 108369, https://doi.org/10.1016/j.jobe.2023.108369.
- [58] M. Lourakis, A brief description of the Levenberg-larquardt mlgorithm implemened by levmar, in: A Brief Description of the Levenberg-Marquardt Algorithm Implemented by Levmar, vol. 4, 2005.
- [59] R. Fletcher, Practical Methods of Optimization, second ed., Wiley, 2000.
- [60] J. Kennedy, R. Eberhart, Particle swarm optimization, in: Proceedings of ICNN'95 International Conference on Neural Networks, vol 4, 1995, pp. 1942–1948, https://doi.org/10.1109/ICNN.1995.488968.
- [61] E. Atashpaz-Gargari, C. Lucas, Imperialist competitive algorithm: an algorithm for optimization inspired by imperialistic competition, in: 2007 IEEE Congress on Evolutionary Computation, 2007, pp. 4661–4667, https://doi.org/10.1109/CEC.2007.4425083.
- [62] A.D. Skentou, A. Bardhan, A. Mamou, M.E. Lemonis, G. Kumar, P. Samui, D.J. Armaghani, P.G. Asteris, Closed-Form equation for estimating unconfined compressive strength of granite from three non-destructive tests using soft computing models, Rock Mech. Rock Eng. 56 (1) (2023) 487–514, https://doi.org/ 10.1007/s00603-022-03046-9.

- [63] A.H. Alavi, A.H. Gandomi, Energy-based numerical models for assessment of soil liquefaction, Geosci. Front. 3 (4) (2012), https://doi.org/10.1016/j.gsf.2011.12.008. Article 4.
- [64] M. Apostolopoulou, D.J. Armaghani, A. Bakolas, M.G. Douvika, A. Moropoulou, P.G. Asteris, Compressive strength of natural hydraulic lime mortars using soft computing techniques, Procedia Struct. Integr. 17 (2019) 914–923, https://doi.org/10.1016/j.prostr.2019.08.122.
- [65] D.J. Armaghani, P.G. Asteris, A comparative study of ANN and ANFIS models for the prediction of cement-based mortar materials compressive strength, Neural Comput. Appl. (2020), https://doi.org/10.1007/s00521-020-05244-4.
- [66] P.G. Asteris, V.G. Mokos, Concrete compressive strength using artificial neural networks, Neural Comput. Appl. (2019), https://doi.org/10.1007/s00521-019-04663-2.
- [67] L. Cavaleri, M.S. Barkhordari, C.C. Repapis, D.J. Armaghani, D.V. Ulrikh, P.G. Asteris, Convolution-based ensemble learning algorithms to estimate the bond strength of the corroded reinforced concrete, Constr. Build. Mater. 359 (2022) 129504, https://doi.org/10.1016/j.conbuildmat.2022.129504.
- [68] S.M. Lundberg, S.-I. Lee, A unified approach to interpreting model predictions, Adv. Neural Inf. Process. Syst. 30 (2017).
- [69] H. Huang, M. Guo, W. Zhang, M. Huang, Seismic behavior of strengthened RC columns under combined loadings, J. Bridge Eng. 27 (6) (2022) 05022005, https://doi.org/10.1061/(ASCE)BE.1943-5592.0001871.
- [70] X. Long, P.M. Iyela, Y. Su, M.M. Atlaw, S.-B. Kang, Numerical predictions of progressive collapse in reinforced concrete beam-column sub-assemblages: a focus on 3D multiscale modeling, Eng. Struct. 315 (2024) 118485, https://doi.org/10.1016/j.engstruct.2024.118485.
- [71] W. Zhang, X. Yang, J. Lin, B. Lin, Y. Huang, Experimental and numerical study on the torsional behavior of rectangular hollow reinforced concrete columns strengthened by CFRP, Structures 70 (2024) 107690, https://doi.org/10.1016/j.istruc.2024.107690.
- [72] D. Gao, Z. Li, C. Ding, Z. Yu, Uniaxial tensile stress-strain constitutive relationship of 3D/4D/5D steel fiber-reinforced concrete, Constr. Build. Mater. 470 (2025) 140539, https://doi.org/10.1016/j.conbuildmat.2025.140539.
- [73] W. Zhang, X. Liu, Y. Huang, M.-N. Tong, Reliability-based analysis of the flexural strength of concrete beams reinforced with hybrid BFRP and steel rebars, Arch. Civ. Mech. Eng. 22 (4) (2022) 171, https://doi.org/10.1007/s43452-022-00493-7.